Cation Charge and Size Selectivity of the C2 Domain of Cytosolic Phospholipase A_2[†]

Eric A. Nalefski[‡] and Joseph J. Falke*

Department of Chemistry and Biochemistry, University of Colorado at Boulder, Boulder, Colorado 80309-0215

Received September 17, 2001; Revised Manuscript Received November 16, 2001

ABSTRACT: C2 domains regulate numerous eukaryotic signaling proteins by docking to target membranes upon binding Ca^{2+}. Effective activation of the C2 domain by intracellular Ca^{2+} signals requires high Ca^{2+} selectivity to exclude the prevalent physiological metal ions K^+, Na^+, and Mg^{2+}. The cooperative binding of two Ca^{2+} ions to the C2 domain of cytosolic phospholipase A_2 (cPLA$_2$-α) induces docking to phosphatidylcholine (PC) membranes. The ionic charge and size selectivities of this C2 domain were probed with representative mono-, di-, and trivalent spherical metal cations. Physiological concentrations of monovalent cations and Mg^{2+} failed to bind to the domain and to induce docking to PC membranes. Superphysiological concentrations of Mg^{2+} did bind but still failed to induce membrane docking. In contrast, Ca^{2+}, Sr^{2+}, and Ba^{2+} bound to the domain in the low micromolar range, induced electrophoretic mobility shifts in native polyacrylamide gels, stabilized the domain against thermal denaturation, and induced docking to PC membranes. In the absence of membranes, the degree of apparent positive cooperativity in binding of Ca^{2+}, Sr^{2+}, and Ba^{2+} decreased with increasing cation size, suggesting that the C2 domain binds two Ca^{2+} or Sr^{2+} ions, but only one Ba^{2+} ion. These stoichiometries were correlated with the abilities of the ions to drive membrane docking, such that micromolar concentrations of Ca^{2+} and Sr^{2+} triggered docking while even millimolar concentrations of Ba^{2+} yielded poor docking efficiency. The simplest explanation is that two bound divalent cations are required for stable membrane association. The physiological Ca^{2+} ion triggered membrane docking at 20-fold lower concentrations than Sr^{2+}, due to both the higher Ca^{2+} affinity of the free domain and the higher affinity of the Ca^{2+}-loaded domain for membranes. Kinetic studies indicated that Ca^{2+} ions bound to the free domain are retained at least 5-fold longer than Sr^{2+} ions. Moreover, the Ca^{2+}-loaded domain remained bound to membranes 2-fold longer than the Sr^{2+}-loaded domain. For both Ca^{2+} and Sr^{2+}, the two bound metal ions dissociate from the protein−membrane complex in two kinetically resolvable steps. Finally, representative trivalent lanthanide ions bound to the domain with high affinity and positive cooperativity, and induced docking to PC membranes. Overall, the results demonstrate that both cation charge and size constraints contribute to the high Ca^{2+} selectivity of the C2 domain and suggest that formation of a cPLA$_2$-α C2 domain−membrane complex requires two bound multivalent metal ions. These features are proposed to stem from the unique structural features of the metal ion-binding site in the C2 domain.

The C2 domain is a eukaryotic membrane-targeting protein module present in numerous signal transducing proteins that carry out key cellular functions at membranes (reviewed in refs *1* and *2*). These processes include the generation of lipid second messengers, vesicular transport, GTPase regulation, protein phosphorylation, pore formation by cytolytic T cells, and ubiquitin-mediated protein degradation. C2 domains bind a variety of cellular targets, including phospholipids, inositol polyphosphates, and other membrane-associated proteins (*1*, *2*). Many of these C2 domains bind to target membranes in response to the micromolar Ca^{2+} levels generated during intracellular Ca^{2+} fluxes. The structures of representative Ca^{2+}-regulated C2 domains, including the C2A domain of synaptotagmin I (Syt-IA),[1] the C2 domain of cytosolic phospholipase A_2 (α-isoform, cPLA$_2$-α), and the C2 domain of protein kinase C (*β*-isoform, PKC-*β*), have been determined by X-ray crystallography and NMR spectroscopy (*3*−*8*). These C2 domains are divided into two distinct topological classes (*1*), both of which are constructed of *β*-sandwich architecture. At one edge of the *β*-sandwich, two or more Ca^{2+} ions bind in an aspartate-lined cleft formed by three interstrand loops. Equilibrium Ca^{2+} binding measurements have shown that the isolated cPLA$_2$-α C2 domain binds two Ca^{2+} ions with low micromolar affinity when free in solution, and with even higher affinity when bound to target phosphatidylcholine (PC) membranes (*7*, *9*). Two Ca^{2+}

[†] Support provided by NIH Grant GM R01-63235 (J.J.F.) and NIH Postdoctoral Fellowship GM-18303 (E.A.N.).

* To whom correspondence should be addressed. Telephone: (303) 492-3503. Fax: (303) 492-5894. E-mail: falke@colorado.edu.

[‡] Current address: U.S. Genomics, Woburn, MA 01801.

[1] Abbreviations: Syt-IA, synaptotagmin I-A; cPLA$_2$-α, cytosolic phospholipase A_2 α; PKC-*β*, protein kinase C *β*; PC, phosphatidylcholine; PAGE, polyacrylamide gel electrophoresis; EDTA, ethylenediaminetetraacetic acid; PIPES, piperazine-*N*,*N*′-bis(2-ethanesulfonic acid); FRET, fluorescence resonance energy transfer; dansyl-PE or dPE, *N*-[5-(dimethylamino)naphthalene-1-sulfonyl]-1,2-dihexadecanoyl-*sn*-glycero-3-phosphoethanolamine; EIR, effective ionic radius; PLC-*δ*1, phospholipase C *δ*1; SEM, standard error of the mean.

10.1021/bi011798h CCC: $22.00 © 2002 American Chemical Society
Published on Web 01/04/2002

ions have also been observed in the crystal structure of the domain (*6*, *8*). The binding of the Ca^{2+} ions is positively cooperative and induces docking of the domain to phosphatidylcholine (PC) membranes (*9*−*11*) such that that the C2 domain is activated over the narrow micromolar range of Ca^{2+} concentrations achieved during intracellular Ca^{2+} signaling. In contrast, three Ca^{2+} ions bind to the Syt-IA and PKC-β C2 domains and induce docking to anionic lipids such as phosphatidylserine (PS). It has become clear that C2 domains exhibit different modes of membrane binding and Ca^{2+} activation parameters adapted for distinct signaling pathways (*12*).

C2 domains regulated by micromolar cytoplasmic Ca^{2+} signals must possess the ability to selectively bind Ca^{2+} in the presence of 10^3−10^4-fold higher concentrations of K^+, Na^+, and Mg^{2+} (*13*). Several studies have indicated that physiological levels of these background cations do not induce binding of Ca^{2+}-dependent C2 domains to target membranes (*11*, *14*, *15*), although a sub-millimolar Mg^{2+} concentration induces membrane binding by the C2A domain of synaptotagmin III (*15*). In addition, spherical divalent cations other than Ca^{2+} induce membrane docking by various C2 domains (*14*−*17*), including cPLA$_2$-α (*11*). In general, the potency of these cations follows this order: $Ca^{2+} > Sr^{2+} > Ba^{2+} \gg Mg^{2+}$. This order of potency also reflects the ability of these ions to promote enzymatic activity of cPLA$_2$-α (*18*). It is not clear, however, whether this cation specificity stems primarily from the metal affinity of the free C2 domain or from the stability of different domain−metal−membrane complexes. In principle, the target membrane could contribute to the observed cation specificity of C2 domains, since (i) target membranes significantly increase the Ca^{2+} affinity of the cPLA$_2$-α, Syt-IA, and PKC-β C2 domains (*12*, *19*), (ii) the membrane surface contacts the Ca^{2+}-binding loops of the C2 domain when docked to target membranes (reviewed in ref *12*), (iii) phospholipid membranes bind divalent cations with selectivity (*20*), and (iv) phospholipid may complete the coordination shell surrounding the exposed bound Ca^{2+} by displacing coordinating water molecules as observed for the C2 domain of PKC-α (*21*). Thus, a complete understanding of the molecular basis of the Ca^{2+} selectivity of the C2 domain requires the evaluation of metal ion binding by the C2 domain in both its membrane-free and -bound states.

This study probed the Ca^{2+}-binding site of the cPLA$_2$-α C2 domain to better define its cation charge and size selectivity. The Ca^{2+}-activated C2 domain is responsible for targeting cPLA$_2$-α to cytoplasmic membranes (*22*−*24*), where its Ca^{2+}-independent catalytic domain liberates arachidonic acid from glycerophospholipids to initiate eicosanoid pathways, including inflammation (*25*−*27*). When Ca^{2+} binds, the intrinsic tryptophan fluorescence of the cPLA$_2$-α C2 domain increases due to structural, electrostatic, or dynamic changes that influence the environment of the sole tryptophan (Trp^{71}) partially buried in the domain (*9*, *12*). This fluorescence increase enables evaluation of the equilibrium and kinetic binding parameters of various metal ions for the cPLA$_2$-α C2 domain in the presence and absence of target membranes. The results presented here demonstrate that spherical monovalent cations and Mg^{2+} are virtually excluded from the site at physiological concentrations, in the absence or presence of target membranes. In contrast, spherical divalent cations (larger than Mg^{2+}) and trivalent cations bind to the site, even in the absence of membranes, and induce membrane docking by the domain. A relationship is observed between the ionic radius and the apparent stoichiometry of divalent cation binding to the isolated C2 domain, as revealed by the Hill coefficient of positive cooperativity. Furthermore, the degree of positive cooperativity is related to the ability of the divalent cation to induce membrane docking, suggesting that the binding of two metal ions is required to induce membrane docking. A model for the formation of a C2 domain−Ca^{2+}−phospholipid complex is discussed.

MATERIALS AND METHODS

Reagents. Chloride salts (>99.5% pure) of mono-, di-, and trivalent metal ions were used (Aldrich or Fluka). According to the manufacturer's specifications, $MgCl_2$ contained <0.001% Ca^{2+}. The PC that was utilized was 1-palmitoyl-2-oleoyl-*sn*-glycero-3-phosphocholine (Avanti Polar Lipids). The dansyl-PE that was utilized was *N*-[5-(dimethylamino)-naphthalene-1-sulfonyl]-1,2-dihexadecanoyl-*sn*-glycero-3-phosphoethanolamine (Molecular Probes).

C2 Domain Production and Isolation. The cPLA$_2$-α C2 domain, spanning the first 138 residues of the human enzyme, was expressed in *Escherichia coli* inclusion bodies, refolded in vitro, and purified as described previously (*9*). Active monomers of the refolded C2 domain were purified by Ca^{2+}-dependent binding to a PC−phenyl Sepharose column, elution with ethylenediaminetetraacetic acid (EDTA), and being passed over a Sephadex G-75 gel filtration column. C2 domain preparations were judged to be >90% pure when analyzed by denaturing polyacrylamide gel electrophoresis (PAGE). Protein was snap-frozen in standard buffer composed of 100 mM KCl and 20 mM piperazine-*N*,*N*′-bis(2-ethanesulfonic acid) (PIPES) (pH 7.0) with KOH, supplemented with 1 mM $CaCl_2$, and stored at −80 °C. Protein was decalcified by being passed over Chelex-100 resin prior to use and quantified by the Bradford assay using a C2 domain standard, the concentration of which was determined by the tyrosinate method (*28*).

Native-PAGE Analysis. The C2 domain was resuspended in standard buffer containing 2 mM EDTA with or without 3 mM divalent cation. Reversibility was tested by chelating divalent cations with an additional 2 mM EDTA after a short incubation. To test the effect of monovalent cations, the C2 domain was resuspended in 20 mM PIPES (pH 7.0) and 2 mM EDTA with or without 200 mM KCl or NaCl. Protein samples were subjected to 15% nondenaturing PAGE and stained with Coomassie Brilliant Blue.

Determination of T_m. The temperature dependence of the intrinsic fluorescence Trp^{71} of the C2 domain was monitored as a measure of the integrity of domain folding (*9*) on an SLM 48000S fluorescence spectrometer in thermostated quartz cuvettes (λ_{ex} = 284 nm, excitation bandwidth = 4 nm, emission bandwidth = 8 nm). Emission of the C2 domain was scanned or monitored at a single wavelength (λ_{em} = 325 nm). To test the effect of monovalent cations, the C2 domain (0.5 μM) was incubated in 20 mM PIPES (pH 7.0) and 1 mM EDTA with or without 100−200 mM KCl or NaCl. To test divalent cations, the C2 domain was incubated in standard buffer containing 1 mM EDTA and 2 mM divalent cations. The temperature was increased step-

wise, allowing the protein to equilibrate 30 min at each temperature before fluorescence was measured. The fraction of the denatured C2 domain (f) was calculated assuming a two-state (native and denatured) model of the protein as (*28*):

$$f = \frac{F - (\alpha + \beta T)}{(\alpha + \beta T) - (\gamma + \delta T)} \quad (1)$$

where F represents the Trp^{71} emission at 325 nm, T is the temperature, and $\alpha + \beta T$ and $\gamma + \delta T$ are the linear temperature-dependent changes in Trp^{71} emission in the native and denatured states, respectively, determined by extrapolation. T_m values, where $f = 0.5$, were calculated as the midpoint of plots of $\ln[f/(1 - f)]$ versus temperature in the linear transition region.

Fluorescence Detection of Cation and Membrane Binding. The intrinsic Trp^{71} fluorescence of the C2 domain (0.5 μM), without or with sonicated vesicles of PC (100 μM), was monitored at 25 °C in standard buffer as described previously (*9*). Buffer-subtracted emission spectra were recorded for samples diluted in standard buffer to which 1 mM $CaCl_2$ and 5 mM EDTA had been sequentially added.

The cation dependence of the fluorescence increase was quantified by monitoring the fluorescence emission (λ_{em} = 325 nm) upon addition of concentrated solutions of cations to the C2 domain in standard buffer. The fluorescence change (ΔF) was plotted as a function of free cation concentration (x) and best-fitted using a modified Hill equation:

$$\Delta F = \Delta F_{max}\left(\frac{x^H}{[\text{cation}]_{1/2}{}^H + x^H}\right) \quad (2)$$

where ΔF_{max} represents the calculated maximal fluorescence change, H represents the Hill coefficient, and $[\text{cation}]_{1/2}$ represents the free cation concentration that induces a half-maximal fluorescence change. ΔF_{max} was normalized to the initial fluorescence intensity of the C2 domain prior to addition of cation (F_0) and expressed as a percentage to compare the relative fluorescence changes induced by saturating amounts of different cations. The reversibility of the cation-induced fluorescence change was demonstrated by addition of excess EDTA upon completion of the titration. Since ΔF did not plateau by 10 mM Mg^{2+} (see Figure 2A), a relative ΔF_{max} of 13% was used for normalization in Mg^{2+} titrations.

C2 domain binding to sonicated vesicles of PC was assessed using fluorescence resonance energy transfer (FRET) as described previously (*9*, *29*). Trp^{71} of the C2 domain was used as a fluorescence donor, and dansyl-PE incorporated into PC vesicles was used as the fluorescence acceptor. FRET was assessed by mixing the C2 domain (0.5 μM) at 25 °C in standard buffer with vesicles of PC containing a small mole fraction of dansyl-PE (PC:dPE lipid mole ratio of 95:5, total lipid concentration of 100 μM). The C2 domain was excited, and fluorescence emission of dansyl-PE was monitored (λ_{ex} = 284 nm; λ_{em} = 520 nm). The change in the FRET signal was analyzed by the Hill equation (eq 2). The reversibility of FRET was demonstrated by addition of excess EDTA at the completion of the titration. Since ΔF did not approach a plateau in Ba^{2+} and Mg^{2+} titrations (see Figure 4A), relative ΔF_{max} values from Ca^{2+} titrations were used for normalization.

Application of the Hill equation to this analysis of fluorescent data is an approximation, first, since the Hill approach was designed to examine the stoichiometric binding of ligands to multiple identical binding sites and, second, since in this case the relative fluorescence changes for multiple binding events is not known. Nevertheless, Hill analysis can offer insight into the binding mechanism by providing an accurate determination of the $[\text{cation}]_{1/2}$ value, the concentration of cation that elicits a half-maximal fluorescence change, which is related to the binding affinity. Moreover, an observed Hill coefficient of >1.4 (and <2) indicates positive cooperativity in cation binding, even when the fluorescence changes that accompany binding of the individual ions are unknown, and thus a stoichiometry of at least two ions (*30*).

The phospholipid dependence of FRET was quantified as described previously (*9*) by mixing the C2 domain (0.5 μM) at 25 °C with 1 mM EDTA and 2 mM divalent cations in standard buffer and monitoring the emission of dansyl-PE upon addition of concentrated stocks of PC vesicles containing dansyl-PE (5% mol/mol). The change in FRET signal (ΔF) due to C2 domain binding was plotted as a function of PC concentration (x) and best-fitted using the equation for a single population of identical sites:

$$\Delta F = \Delta F_{max}\left(\frac{x}{K_D^{PC} + x}\right) \quad (3)$$

where K_D^{PC} represents the apparent equilibrium dissociation constant of the C2 domain for PC in the presence of approximately 1 mM free divalent cation. In these experiments, the concentration of the C2 domain was small compared to the calculated K_D^{PC}; thus, the total concentration of PC was taken as the free concentration. Since ΔF did not approach a plateau during Ba^{2+} and Mg^{2+} titrations (see Figure 4B), relative ΔF_{max} values from Ca^{2+} titrations were used for normalization.

For all equilibrium fluorescence experiments, buffers, plasticware, and quartz cuvettes were decalcified prior to use as described previously (*31*). Using these procedures, levels of Ca^{2+} contamination in the sample solutions were estimated to be no more than 0.3 μM in equilibrium fluorescence experiments (data not shown), as determined by the fluorescent Ca^{2+} chelator Quin-2. In experiments in which the properties of the C2 domain in the presence of PC vesicles and Ca^{2+} at pH 7.0 were monitored, total Ca^{2+} levels required only small corrections for both Ca^{2+} contamination and the small fraction of the Ca^{2+} population bound to the C2 domain (assuming a stoichiometry of two ions per domain) to obtain free Ca^{2+} levels at each step in the titration. Previously, little or no binding of Ca^{2+} to PC vesicles (2 mM) was demonstrated by equilibrium dialysis (*9*), obviating corrections for Ca^{2+} binding to the membranes themselves. Because of the lower affinities of the other divalent cations, total ion levels were taken as free levels. Assays testing the binding of trivalent cations were carried out in 100 mM KCl and 20 mM PIPES (pH 6.0) (see the Results).

Large Phospholipid Vesicle Binding Assay. C2 domain binding to large multilamellar phospholipid vesicles was assessed as described previously (*11*). Briefly, the C2 domain in standard buffer containing 1 mM EDTA and 2 mM divalent cations was incubated in suspensions of pure PC

membranes prepared by brief sonication. Unbound C2 domain was separated from membrane-bound material by centrifugation. Bound and unbound fractions were subjected to SDS−PAGE, stained with Coomassie Brilliant Blue, and quantified by densitometry. The amount of C2 domain bound to phospholipid was calculated as the percentage of total supernatant and pellet C2 domain present in pellet fractions.

Stopped-Flow Fluorescence Spectroscopy. Stopped-flow fluorescence spectroscopy was carried out on an Applied Photophysics model 17MV stopped-flow spectrofluorometer in standard buffer at 25 °C as described previously (*9*). The dead time of the instrument was determined to be ~1.5 ms (*32*); hence, data collected during the first 1.5 ms were omitted from analysis. To measure the time course of Trp^{71} changes in the C2 domain upon cation dissociation, the C2 domain (5 μM), diluted in 100 μM divalent cation with or without vesicles of PC (250 μM), was rapidly mixed with 5 mM EDTA. The intrinsic fluorescence of Trp^{71} in the C2 domain was recorded using a λ_{ex} of 284 nm and a 335 nm high-pass filter. To measure the time course of FRET between the C2 domain and membranes, the C2 domain (5 μM), diluted in 100 μM divalent cation with vesicles (250 μM total lipid composed of a 95:5 PC/dPE mixture), was rapidly mixed with 5 mM EDTA; the fluorescence of dansyl-PE was recorded using a λ_{ex} of 284 nm and a 475 nm high-pass filter. Four thousand data points were collected over 0.1 s for rapid time courses and over 5 s for slow time courses. The fluorescence (F) was plotted as a function of time (t) and was best-fitted by equations for mono- or biexponential decay processes as described previously (*9*). The monoexponential decay process is given by

$$F(t) = \Delta F e^{-kt} + C \quad (4)$$

where k is the rate constant of the event monitored, ΔF is the fluorescence amplitude, and C is the intrinsic voltage offset of the stopped-flow experiment. The biexponential sequential decay process is described by

$$F(t) = (\Delta F_1 + \Delta F_2)\left[\left(\frac{\Delta F_1}{\Delta F_1 + \Delta F_2}\frac{k_1}{k_2 - k_1} - \frac{k_1}{k_2 - k_1}\right)e^{-k_2 t} - \left(\frac{\Delta F_1}{\Delta F_1 + \Delta F_2}\frac{k_1}{k_2 - k_1} - \frac{k_2}{k_2 - k_1}\right)e^{-k_1 t}\right] + C \quad (5)$$

where k_1 and k_2 are the rate constants of the first- and second-order events, respectively, and ΔF_1 and ΔF_2 are the fluorescence amplitudes of these steps, respectively. Experiments in which Quin-2 was used to monitor cation release from the C2 domain were carried out as previously described (*9*).

RESULTS

Strategy. The $cPLA_2$-α C2 domain binds two Ca^{2+} ions and forms a kinetically stable complex with PC membranes in vitro at physiological concentrations of Ca^{2+} (*9*). In EDTA buffering systems that maintain known free cation concentrations, the $cPLA_2$-α C2 domain prefers Ca^{2+} over other group IIA cations for the induction of membrane docking (*11*), a property displayed by other C2 domains (*14*−*17*). The study presented here probed the Ca^{2+}-binding site of the C2 domain with monovalent group IA, divalent group IIA, and representative trivalent cations to better define its charge and size selectivity in both the absence and presence of target membranes. All of these cations possess filled outer electronic subshells and thus can be treated as simple hard spheres whose optimal coordination is defined by ligand packing constraints, rather than by a preferred coordination geometry (*33*). Due to the tendency of trivalent lanthanide ions to form insoluble hydroxide complexes, experiments with lanthanide ions were carried out at a lower pH (6.0 compared to 7.0, which was used for other cations) and are discussed separately at the end of the Results.

Effects of Cations on the Electrophoretic Mobility and Stability of the Free Domain. Binding of Ca^{2+} to the free $cPLA_2$-α C2 domain quantitatively shifted its electrophoretic mobility in native PAGE (data not shown and refs *9* and *24*). The shift induced by Ca^{2+} retarded the migration of the anionic C2 domain toward the positive electrode. When excess EDTA was added to the sample prior to electrophoresis, the mobility shifted back to approximately that of the C2 domain incubated with EDTA alone. Both Sr^{2+} and Ba^{2+} induced a comparable mobility shift, whereas Mg^{2+} and 200 mM KCl and NaCl failed to induce this mobility shift (data not shown). These results indicate that the binding of Ca^{2+}, Sr^{2+}, and Ba^{2+} alters the size, shape, or charge of the $cPLA_2$-α C2 domain, whereas the binding of Mg^{2+}, K^+, or Na^+ cannot be detected by this assay.

The level of stabilization of the free $cPLA_2$-α C2 domain by the binding of cations was measured as an increase in the melting temperature (T_m) of the C2 domain upon addition of 1 mM free divalent cation (Figure 1). The T_m for thermal denaturation was determined by monitoring the intrinsic fluorescence of Trp^{71} in the $cPLA_2$-α C2 domain, which red shifts and is partially quenched when the domain unfolds in the presence of chemical denaturants (*11*) or at increased temperatures (Figure 1A). Thermal denaturation curves were analyzed using eq 1, assuming a two-state model in which a unique native state is converted to a single unfolded state (Figure 1B). The average T_m (±SEM, $n = 3$) of the C2 domain, which was 46.4 ± 0.1 °C in the absence of divalent cations, increased to 64.9 ± 0.7 °C in the presence of Ca^{2+}. Similar T_m values and increases in T_m by Ca^{2+} binding have been reported for the C2A domain of synaptotagmin I using circular dichroism (*34*). Ca^{2+} binding has also been shown to increase the T_m of the PKC-α C2 domain measured by Fourier transform infrared spectroscopy (*35*). Sr^{2+} and Ba^{2+} increased the T_m of the C2 domain to 56.7 ± 0.6 and 58.0 ± 0.5 °C, respectively, whereas Mg^{2+} had no effect (T_m = 46.1 ± 0.2 °C). In addition, 200 mM K^+ or Na^+ had no effect on T_m (data not shown). These results indicate that the binding of Ca^{2+}, Sr^{2+}, or Ba^{2+} stabilizes the folded C2 domain against thermal denaturation, while the binding of Mg^{2+}, K^+, and Na^+ was not detected by this assay. The greater enhancement in T_m induced by Ca^{2+} over Sr^{2+} and Ba^{2+} is likely to indicate a higher affinity of Ca^{2+} at elevated temperatures or a greater intrinsic stability of the Ca^{2+}-occupied state.

Cation-Induced Intrinsic Fluorescence Changes in the Absence and Presence of Membranes. The ability of Ca^{2+} to bind to the $cPLA_2$-α C2 domain, in both the absence and presence of target membranes, was measured using the intrinsic Trp^{71} of the domain as a probe. The Ca^{2+} dependencies of the intrinsic Trp^{71} changes were previously

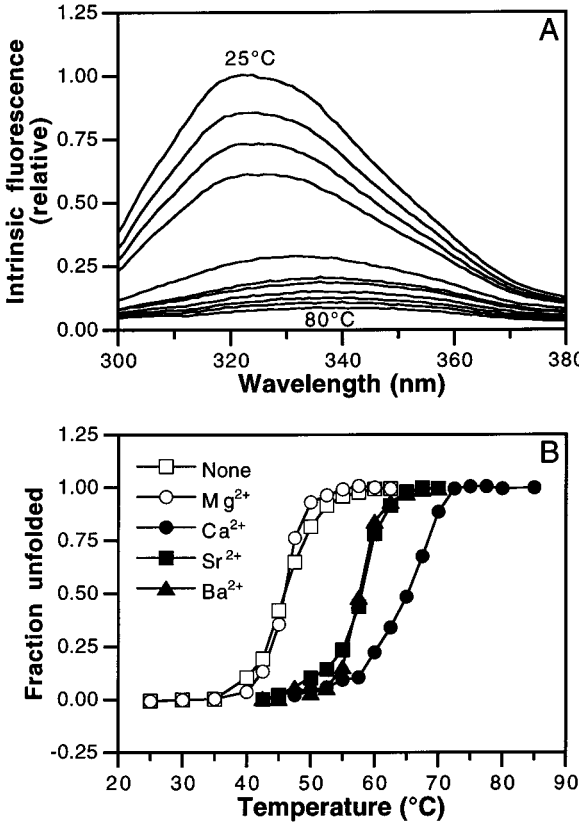

FIGURE 1: Group IIA cations stabilize the cPLA$_2$-α C2 domain against thermal denaturation. (A) Buffer-subtracted intrinsic emission spectra of the C2 domain without added divalent cation, recorded at ~5 °C intervals between 25 and 80 °C. (B) Thermal unfolding of the C2 domain measured by monitoring Trp^{71} emission (λ_{em} = 325 nm) in the presence of no added divalent cation [none (□)] or one of the following: 2 mM total Mg^{2+} (○), Ca^{2+} (●), Sr^{2+} (■), or Ba^{2+} (▲). T_m values were calculated at the midpoints of the linear transitions (see Materials and Methods), and 200 mM Na^+ and K^+ had no effect on T_m values (data not shown). Experimental conditions for both panels A and B: 100 mM KCl, 20 mM PIPES, pH 7.0, and 1 mM EDTA (λ_{ex} = 284 nm).

demonstrated to be strikingly similar to the binding of Ca^{2+} assessed directly by equilibrium dialysis, suggesting that the environmental changes detected by Trp^{71} are directly coupled to the cooperative binding of two Ca^{2+} ions (*9*). As observed previously (*9*, *12*, *36*), Ca^{2+} induced an increase in Trp^{71} fluorescence, which was reversed upon chelation of Ca^{2+} by addition of excess EDTA. In the presence of PC vesicles, Ca^{2+} elicited an even greater increase in Trp^{71} fluorescence, which was also reversed by EDTA addition. Thus, both Ca^{2+} binding and membrane docking induce changes in the domain that alter the environment of Trp^{71}. Addition of up to 100 mM Na^+ or 200 mM K^+ failed to significantly alter Trp^{71} fluorescence in the absence or presence of vesicles (data not shown), demonstrating that physiological concentrations of these monovalent cations do not cause detectable environmental changes at this location.

The same assay was used to quantitatively compare the binding of Ca^{2+} and other group IIA cations to the cPLA$_2$-α C2 domain, in both the presence and absence of target membranes (Figure 2). The fluorescence changes (ΔF) were plotted against free cation concentration and fitted with the Hill equation (eq 2) to determine $[cation]_{1/2}$, the concentration of cation that induces a half-maximal fluorescence change, the Hill coefficient (H), a constant related to cation stoichi-

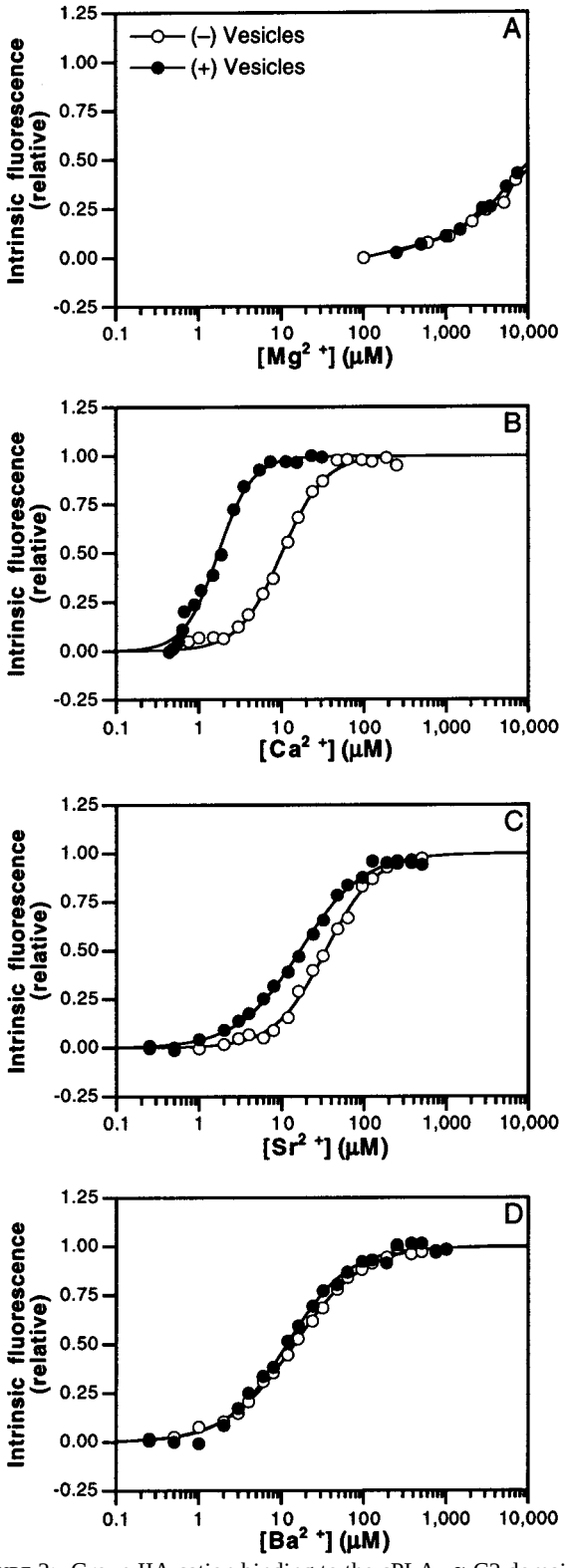

FIGURE 2: Group IIA cation binding to the cPLA$_2$-α C2 domain is selective. Intrinsic fluorescence changes in Trp^{71} of the C2 domain induced by the indicated divalent cations in the absence (white symbols) or presence (black symbols) of PC vesicles (100 μM PC). Fluorescence emission of Trp^{71} was monitored. The observed fluorescence change (ΔF) was normalized to the calculated maximal cation-induced fluorescence change (ΔF_{max}). Solid lines represent the fitting to the Hill equation (eq 2), except for Mg^{2+} titration; equilibrium parameters are summarized in Table 1. Cation-induced increases in intrinsic fluorescence were reversed by addition of excess EDTA at the completion of the titrations (not shown). Experimental conditions: 100 mM KCl, 20 mM PIPES, pH 7.0, and 25 °C (λ_{ex} = 284 nm; λ_{em} = 325 nm).

Table 1: Equilibrium Parameters for Events Driven by Divalent Cation Binding to the cPLA$_2$-α C2 Domain[a]

	cation binding[b]						cation requirement for membrane binding[c]		membrane binding[d]
	without vesicles			with vesicles					
cation	[cation]$_{1/2}$ (μM)	Hill coefficient	normalized ΔF_{max} (%)	[cation]$_{1/2}$ (μM)	Hill coefficient	normalized ΔF_{max} (%)	[cation]$_{1/2}$ (μM)	Hill coefficient	K_D^{PC} (μM)
Mg^{2+}	>10000 [e]	ND[f]	ND[f]	>10000[e]	ND[f]	ND[f]	≫10000[g]	ND[f]	≫100[g]
Ca^{2+}	11 ± 2	1.8 ± 0.1	13 ± 1	2 ± 1	1.8 ± 0.2	25 ± 1	2 ± 1	1.9 ± 0.2	11 ± 1
Sr^{2+}	31 ± 2	1.4 ± 0.1	13 ± 1	18 ± 2	1.2 ± 0.1	22 ± 2	43 ± 1	1.2 ± 0.1	40 ± 3
Ba^{2+}	14 ± 2	1.0 ± 0.1	12 ± 1	15 ± 3	1.0 ± 0.1	12 ± 1	>2000[e]	ND[f]	>170[e]

[a] Results are expressed as averages ± SEM ($n = 3$). Experimental conditions: 100 mM KCl, 20 mM PIPES, pH 7.0, and 25 °C. [b] Determined by monitoring the intrinsic Trp[71] fluorescence of the C2 domain in the absence or presence of PC vesicles (100 μM phospholipid), as described in the legend of Figure 2. Data analyzed by fitting to the Hill equation (eq 2). [c] Determined by monitoring protein to membrane FRET in the presence of PC/dansyl-PE vesicles (95:5, 100 μM phospholipid), as described in the legend of Figure 4A. Data analyzed by fitting to the Hill equation (eq 2). [d] Determined by monitoring protein to membrane FRET using PC/dansyl-PE vesicles (95:5), as described in the legend of Figure 4B. Data analyzed by fitting to the independent site equation (eq 3). [e] The value is a lower limit estimate of the titration midpoint since the observed fluorescence change did not plateau. [f] Not determined due to insufficient affinity. [g] No binding observed at this ligand concentration.

ometry and cooperativity (see Materials and Methods), and ΔF_{max} (Table 1). In the absence of membranes, Mg^{2+} at >1 mM increased Trp[71] fluorescence, indicating that this small divalent cation can bind to the free C2 domain at superphysiological concentrations; however, the apparent affinity was too low to achieve plateau values even at 10 mM Mg^{2+}. Thus, a lower limit for the $[Mg^{2+}]_{1/2}$ value was placed at 10 mM. In contrast, Ca^{2+}, Sr^{2+}, and Ba^{2+} bound to the free C2 domain at much lower concentrations, yielding [cation]$_{1/2}$ values of 11, 31, and 14 μM, respectively. Ca^{2+}, Sr^{2+}, and Ba^{2+} induced similar maximal fluorescence increases (normalized $\Delta F_{max} = 12-13\%$). The Hill coefficient decreased as ionic size increased, calculated as 1.8, 1.4, and 1.1 for Ca^{2+}, Sr^{2+}, and Ba^{2+}, respectively. Given that this C2 domain is known to bind only two Ca^{2+} ions (*6*, *7*, *9*), these apparent Hill values strongly suggest that two Ca^{2+} and Sr^{2+} ions bind to the free C2 domain in a positively cooperative manner but that only one Ba^{2+} ion binds to the domain in the micromolar range.

In the presence of PC membranes, the [cation]$_{1/2}$ value decreased for both Ca^{2+} (to 1.6 μM) and Sr^{2+} (to 18 μM) but was unchanged for Mg^{2+} and Ba^{2+} (Figure 2 and Table 1). In addition, maximal fluorescence changes increased for only Ca^{2+} and Sr^{2+} (to 25 and 22%, respectively) but not for Ba^{2+} ($\Delta F_{max} = 12\%$), suggesting that only Ca^{2+} and Sr^{2+} induce membrane docking at low ion concentrations. In the presence of PC membranes, Hill coefficients of 1.8, 1.2, and 1.0 were observed for Ca^{2+}, Sr^{2+}, and Ba^{2+}, respectively; all of these coefficients were similar to their values in the absence of membranes. Together, these results suggest that although the Ca^{2+}-binding site of the cPLA$_2$-α C2 domain can accommodate the larger group IIA cations Ca^{2+}, Sr^{2+}, and Ba^{2+}, only the Ca^{2+} and Sr^{2+} ions bind with a stoichiometry of two per domain and trigger membrane docking. By contrast, Ba^{2+} appears to bind with a stoichiometry of one per domain and fails to drive membrane association.

Cation-Induced Membrane Binding. The ability of group IIA cations to induce the binding of the cPLA$_2$-α C2 domain to target membranes was further tested in a direct centrifugation assay (Figure 3). This assay revealed that Ca^{2+}, and to a lesser extent Sr^{2+}, promotes the binding of the C2 domain to large vesicles of PC. Little or no binding of the C2 domain to PC vesicles was observed in the absence of divalent cations or in the presence of Mg^{2+} or Ba^{2+}.

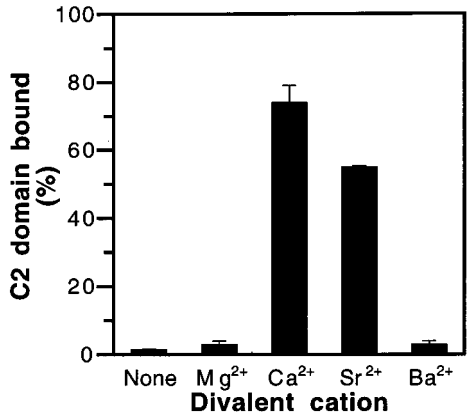

FIGURE 3: Group IIA cations induce selective binding of the cPLA$_2$-α C2 domain to large vesicles. The C2 domain was incubated with PC vesicles without (none) or with the indicated divalent cation at 2 mM. C2 domain bound to the vesicles was separated from unbound protein by centrifugation. Supernatant and the pelleted vesicle fraction were analyzed by 15% SDS−PAGE and quantified by staining with Coomassie Brilliant Blue. Results are expressed as the fraction of the total protein that is present in the pellet. Bars are averages of three independent determinations; error bars represent standard errors of the mean. Experimental conditions: 100 mM KCl, 20 mM PIPES, pH 7.0, 1 mM EDTA, and room temperature.

The cation selectivity of the cPLA$_2$-α C2 domain for docking to target membranes was measured more quantitatively using a fluorescence resonance energy transfer (FRET) assay (Figure 4). Ca^{2+}-induced membrane docking results in transfer of the donor Trp[71] fluorescence from the C2 domain to the acceptor dansyl-PE fluorophore in 95:5 PC/dPE membranes (data not shown). Such FRET requires the proximity of the Trp[71] and the dansyl-PE probes that exists during the docking of the C2 domain to membranes [R_0 = 21 Å (*37*)]. The increase in acceptor dansyl-PE emission by FRET was reversed by addition of EDTA, demonstrating the reversibility of the FRET signal upon disruption of the protein−membrane complex by Ca^{2+} chelation. Addition of up to 200 mM Na^+ and K^+ (data not shown) and up to 10 mM Mg^{2+} failed to elicit significant FRET (Figure 4A). These results indicate that physiological concentrations of Ca^{2+}, but not K^+, Na^+, and Mg^{2+}, induce docking of the C2 domain to target membranes.

The concentration-dependent FRET signals elicited by Ca^{2+}, Sr^{2+}, and Ba^{2+} were fitted with the Hill equation (eq 2) (Figure 4A and Table 1). The [cation]$_{1/2}$ values of 2.2

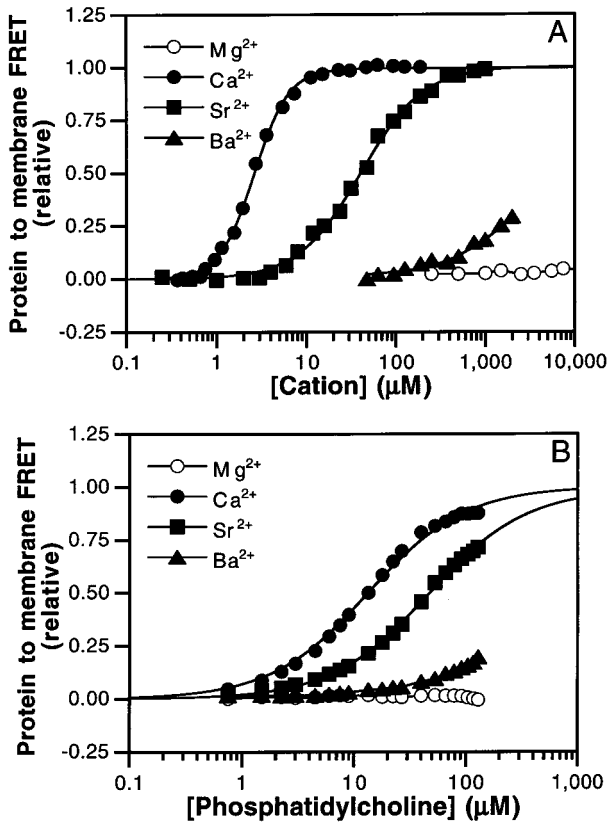

FIGURE 4: Group IIA cations selectively induce docking of the cPLA$_2$-α C2 domain to PC membranes. (A) Divalent cation dependence of C2 domain docking to PC membranes containing dansyl-PE as assessed by protein to membrane FRET. The observed FRET change (ΔF) was fitted (—) with the Hill equation (eq 2) and normalized to the calculated maximal cation-induced FRET change (ΔF_{max}); best-fit parameters are summarized in Table 1. Cation-induced FRET signals were reversed by addition of excess EDTA at the completion of the titration (not shown). Experimental conditions: 100 mM KCl, 20 mM PIPES, pH 7.0, 100 μM PC/dansyl-PE (95:5), and 25 °C (λ_{ex} = 284 nm; λ_{em} = 520 nm). (B) Phospholipid dependence of protein to membrane FRET. The FRET change (ΔF) arising from the C2 domain was normalized to the calculated maximal Ca^{2+}-induced FRET change (ΔF_{max}) and fitted with the single-site equation (eq 3); best-fit parameters are given in Table 1. No concentration-dependent increases in the FRET signal were obtained with the C2 domain without added divalent cation (data not shown). Cation-induced FRET increases were reversed by addition of excess EDTA at the completion of the titrations (not shown). Experimental conditions: 100 mM KCl, 20 mM PIPES, pH 7.0, 2 mM divalent cation, 1 mM EDTA, 95:5 PC/dansyl-PE, and 25 °C (λ_{ex} = 284 nm; λ_{em} = 520 nm).

and 43 μM were observed for the induction of membrane docking by Ca^{2+} and Sr^{2+}, respectively (Table 1). These values are very similar, within 2.3-fold, to the corresponding values measured by monitoring Trp^{71} fluorescence changes, indicating the direct coupling between Ca^{2+} binding and membrane docking. Furthermore, the Hill coefficients of 1.9 and 1.2 measured by FRET for Ca^{2+} and Sr^{2+}, respectively, are the same within error as those obtained in the Trp^{71} fluorescence assay. Notably, the FRET results placed the lower limit for $[Ba^{2+}]_{1/2}$ at 2 mM, since at this concentration of Ba^{2+} the binding of the C2 domain to PC membranes was not yet half-complete. These results indicate that divalent cations differ in their ability to induce membrane docking of the C2 domain to target membranes. Ca^{2+} is 20-fold more potent than Sr^{2+}, at least 1000-fold more potent than Ba^{2+}, and at least 5000-fold more potent than Mg^{2+}. The higher potency of Ca^{2+} relative to Sr^{2+} stems from both the higher Ca^{2+} affinity of the free domain and the higher membrane affinity of the Ca^{2+}-occupied domain (Table 1).

The cation selectivity of the cPLA$_2$-α C2 domain was further investigated by measuring the PC dependence of membrane docking induced by saturating concentrations of divalent cations (Figure 4B and Table 1). This FRET experiment measures the apparent dissociation constant of the cPLA$_2$-α C2 domain for PC (K_D^{PC}) in the presence of 1 mM free group IIA cations (eq 3), a concentration at which the free C2 domain is saturated with divalent cations that induce Trp^{71} fluorescence changes (see Figure 2). The affinity of the C2 domain for target membranes was greatest in the presence of Ca^{2+}, where the apparent dissociation constant for PC (K_D^{PC} = 11 μM) was 4-fold smaller than in the presence of Sr^{2+} (K_D^{PC} = 40 μM) and at least 15-fold smaller than in the presence of Ba^{2+} for which only a lower limit could be measured ($K_D^{PC} \geq 170$ μM). In contrast, at >100 μM PC, no binding of the C2 domain to target membranes was observed in the presence of Mg^{2+} or in the absence of divalent cations (*9*). Calculated normalized ΔF_{max} values were identical for Ca^{2+} and Sr^{2+} (data not shown), confirming that the concentrations of Ca^{2+} and Sr^{2+} that were used were saturating, able to drive equivalent amounts of the C2 domain onto target vesicles, and that the C2 domain displays higher affinity for PC membranes when loaded with Ca^{2+} than when loaded with Sr^{2+}. These results further demonstrate that membrane docking by the cPLA$_2$-α C2 domain is preferentially induced by Ca^{2+} over other group IIA cations and that only Sr^{2+} exhibits the ability to efficiently replace Ca^{2+}.

Kinetics of Divalent Cation Dissociation. Stopped-flow fluorescence spectroscopy was employed to examine the kinetic parameters responsible for the enhanced affinity of the cPLA$_2$-α C2 domain for Ca^{2+} over other group IIA cations (Figure 5 and Table 2). In these experiments, a solution containing the C2 domain, in the presence or absence of PC membranes, and 100 μM divalent cation was rapidly mixed by stopped-flow methods with a solution containing excess EDTA to rapidly bind free cations. The decay in the intrinsic Trp^{71} signal was monitored to measure the environmental changes in the C2 domain that are coupled to irreversible cation dissociation. Previously, we showed that the rate constants for Trp^{71} fluorescence changes in the domain induced by Ca^{2+} chelation were very similar, within 1.7-fold, to the rate constants for Ca^{2+} release directly measured using the fluorescent Ca^{2+} chelator Quin-2 (*9*). Thus, monitoring Trp^{71} emission upon cation chelation with EDTA allows an accurate assessment of an irreversible release of bound cations. In the absence of PC membranes, the time courses of release of group IIA cations from the cPLA$_2$-α C2 domain were best-fitted with monoexponential equations (eq 4). The rate constants for release of Sr^{2+} and Ba^{2+} from the free C2 domain (>560 and >630 s^{-1}, respectively) were considerably larger than that for Ca^{2+} (108 s^{-1}) (Table 2).

To directly monitor the release of group IIA cations from the free C2 domain, EDTA was replaced with Quin-2, which also binds Sr^{2+} and Ba^{2+}. At 25 °C, the fluorescence response of Quin-2 binding to these cations was too low to obtain an adequate fluorescence signal. However, at a reduced tem-

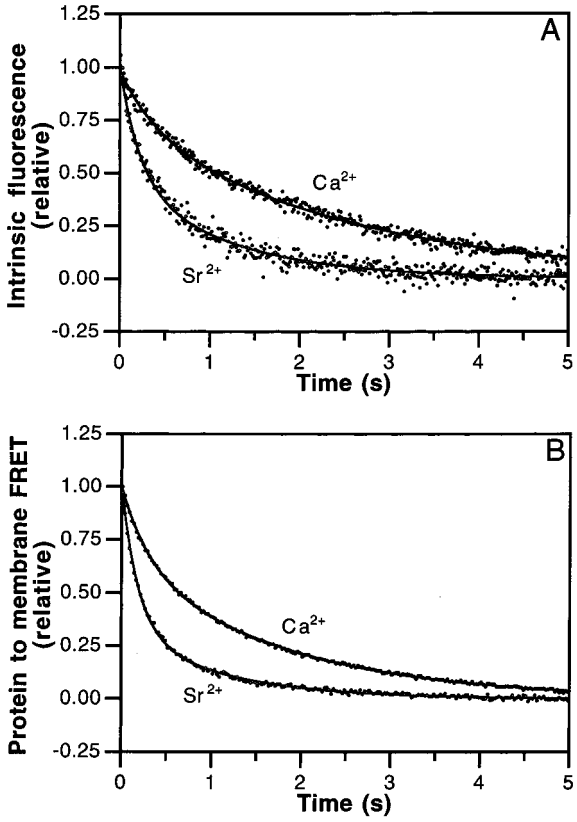

FIGURE 5: Dissociation kinetics of complexes containing the cPLA$_2$-α C2 domain, divalent cations, and membranes. (A) Kinetics of divalent cation dissociation from the membrane-bound C2 domain complex as measured by stopped-flow fluorescence spectroscopy. Solutions of the C2 domain (5 μM) in Ca^{2+} or Sr^{2+} (100 μM) with vesicles of PC (250 μM) were rapidly mixed with 5 mM EDTA. The intrinsic Trp^{71} fluorescence of the C2 domain was monitored using a λ_{ex} of 284 nm and a 335 nm high-pass emission filter. The time courses of fluorescence decays were fitted with the ordered-sequential equation (eq 5) and normalized (—). (B) Decay of the protein-to-membrane FRET signal upon divalent cation dissociation. Solutions of the C2 domain (5 μM) in Ca^{2+} or Sr^{2+} (100 μM) and PC/dansyl-PE vesicles (95:5; 250 μM) were rapidly mixed with 5 mM EDTA. The fluorescence of dansyl-PE was monitored using a λ_{ex} of 284 nm and a 475 nm high-pass emission filter. Solid lines represent the best fits of normalized fluorescence decays to the ordered-sequential equation (eq 5). Results in panels A and B are summarized in Table 2. Experimental conditions: 100 mM KCl, 20 mM PIPES, pH 7.0, and 25 °C.

perature (4 °C), the enhanced fluorescence signal of Quin-2 was sufficient to permit determination of rate constants (data not shown). As was the case at 25 °C, at 4 °C the rate constants for the release of Sr^{2+} (170 ± 20 s^{-1}, $n = 8$) and Ba^{2+} (290 ± 70 s^{-1}, $n = 3$) were still considerably greater than that for Ca^{2+} (14.5 ± 0.1 s^{-1}, $n = 3$). These rate constants were independently confirmed by monitoring Trp^{71} emission upon chelation with EDTA (data not shown); at 4 °C, the rate constants for the release of Sr^{2+} (150 ± 20 s^{-1}, $n = 3$) and Ba^{2+} (250 ± 20 s^{-1}, $n = 3$) were also greater than that for Ca^{2+} (15.1 ± 0.1 s^{-1}, $n = 3$). Together, these results indicate that Ca^{2+} dissociates ~10-fold more slowly from the free cPLA$_2$-α C2 domain than do the larger Sr^{2+} and Ba^{2+} ions, and that the Trp^{71} fluorescence assay faithfully reports either the dissociation of metal ions or a very fast conformational change directly coupled to metal dissociation.

Cation release from the membrane-bound cPLA$_2$-α C2 domain was also assessed by monitoring Trp^{71} fluorescence

Table 2: Kinetic Parameters for Events Triggered by Divalent Cation Dissociation from the cPLA$_2$-α C2 Domain[a]

		cation dissociation[b]		protein-to-membrane FRET[c]	
cation	treatment	k (s^{-1})	ΔF_{rel} (%)	k (s^{-1})	ΔF_{rel} (%)
Ca^{2+}	without vesicles	108 ± 2	NA[d]	NA[d]	NA[d]
	with vesicles				
	step 1	2.5 ± 0.2	40 ± 2	3.1 ± 0.2	45 ± 2
	step 2	0.41 ± 0.02	60 ± 2	0.54 ± 0.02	55 ± 2
Sr^{2+}	without vesicles	>560 ± 90[e]	NA[d]	NA[d]	NA[d]
	with vesicles				
	step 1	3.9 ± 0.3	65 ± 2	5.8 ± 0.6	68 ± 4
	step 2	0.69 ± 0.07	35 ± 2	1.1 ± 0.3	32 ± 4
Ba^{2+}	without vesicles	>630 ± 160[e]	NA[d]	NA[d]	NA[d]
	with vesicles	ND[f]	ND[f]	ND[f]	ND[f]

[a] Determined by stopped-flow fluorescence spectroscopy as described in the legend of Figure 5, analyzed by fitting to a single-exponential equation (without vesicles) (eq 4) or to an ordered-sequential equation (with vesicles) (eq 5). Results expressed as averages ± SEM ($n = 3$). Experimental conditions: 100 mM KCl, 20 mM PIPES, pH 7.0, and 25 °C. [b] Determined by monitoring the intrinsic Trp^{71} fluorescence of the C2 domain, as described in the legend of Figure 5A. [c] Determined by monitoring the decay of protein to membrane FRET, as described in the legend of Figure 5B. [d] Not applicable. [e] Value a lower limit estimate of k since a majority of the fluorescence change occurred during the dead time of the instrument. [f] Not determined.

(Figure 5A and Table 2). Ca^{2+} release from the membrane-bound domain followed a sequential time course consisting of two steps (eq 5) with amplitudes representing 40 and 60% (steps 1 and 2, respectively) of the total fluorescence change (see ΔF values in Table 2). The two rate constants that were measured (2.5 and 0.41 s^{-1}) were similar to those reported previously, which agree well with the sequential dissociation rate constants for two Ca^{2+} ions determined with Quin-2 (*9*). Similarly, Sr^{2+} release from the membrane-bound domain also followed a two-step process (Figure 5A). The rate constants for the two events (3.9 and 0.69 s^{-1}) were each nearly 2-fold greater than those measured for Ca^{2+} and corresponded to 65 and 35% of the total fluorescence change, respectively. The rate constant for Ba^{2+} dissociation in the presence of PC membranes was not measured since little Ba^{2+}-induced membrane binding was observed in equilibrium experiments (see Figure 4). Notably, although Ca^{2+} dissociates 2-fold more slowly than Sr^{2+} from the membrane-bound domain, this difference is not sufficient to explain the 9−20-fold greater efficacy of Ca^{2+} in driving the membrane docking reaction (Table 1).

The kinetics of C2 domain dissociation from the membrane were directly measured by monitoring the decay in protein-to-membrane FRET upon rapidly mixing a solution of the cPLA$_2$-α C2 domain, 100 μM Ca^{2+} or Sr^{2+}, and 95:5 PC/dPE membranes with a solution of EDTA (Figure 5B and Table 2). The FRET time courses were best-fitted with a biexponential equation representing a sequential dissociation process (eq 5). For Ca^{2+}, the rate constants that were measured (3.1 and 0.54 s^{-1}) were similar to those measured previously and agree well with the sequential dissociation rate constants for two Ca^{2+} ions and their accompanying changes in Trp^{71} emission (*9*). Both Sr^{2+} dissociation rate constants (5.8 and 1.1 s^{-1}) were nearly 2-fold greater than those for Ca^{2+}. These results indicate that, as previously observed for the Ca^{2+}-occupied membrane-bound domain (*9*), the Sr^{2+}-occupied membrane-bound domain loses one

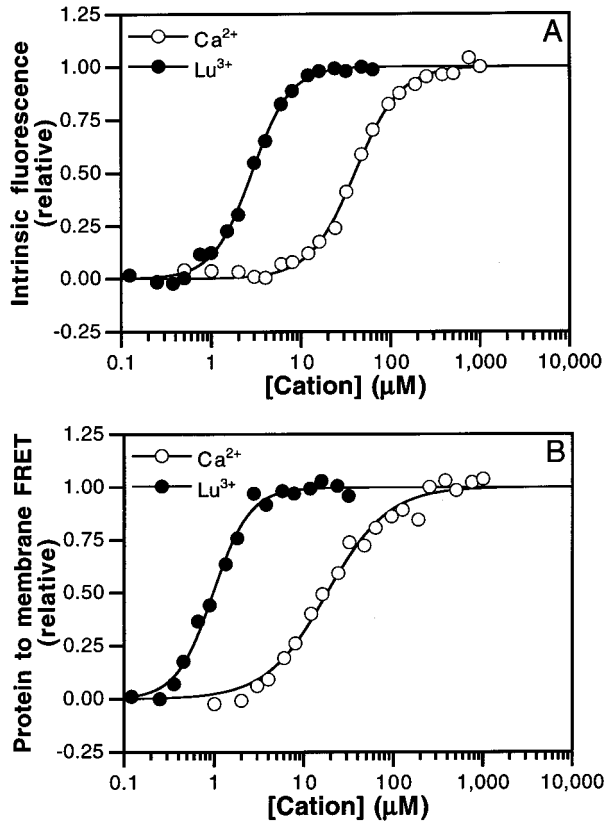

FIGURE 6: Trivalent cations bind to the cPLA$_2$-α C2 domain and induce membrane docking. (A) Intrinsic fluorescence changes in Trp^{71} of the C2 domain induced by Lu^{3+} (black symbols) or Ca^{2+} (white symbols) in the absence of membranes. Fluorescence emission of Trp^{71} was monitored (λ_{em} = 325 nm). The observed fluorescence change (ΔF) was normalized to the calculated maximal cation-induced fluorescence change (ΔF_{max}). Solid lines represent fitting to the Hill equation (eq 1). Results are summarized in the text. (B) Cation dependence of C2 domain docking to PC membranes containing dansyl-PE measured by protein to membrane FRET (λ_{em} = 520 nm). The observed FRET change (ΔF) in response to Lu^{3+} (black symbols) or Ca^{2+} (white symbols) was fitted (—) with the Hill equation (eq 2) and normalized to the calculated maximal cation-induced FRET change (ΔF_{max}). Results are summarized in the text. Experimental conditions: 100 mM KCl, 20 mM PIPES, pH 6.0, and 25 °C (λ_{ex} = 284 nm).

ion but remains docked to the membrane, and then loses the second ion during or shortly after membrane dissociation. Moreover, the higher membrane affinity of the Ca^{2+}-loaded domain relative to that of the Sr^{2+}-loaded domain stems at least partly from its 2-fold longer membrane-bound lifetime.

Binding of Representative Trivalent Cations. The ability of representative trivalent cations, including the lanthanide Lu^{3+}, to bind to the cPLA$_2$-α C2 domain and to induce docking to target membranes was tested at pH 6.0 due to the tendency to form insoluble hydroxides at higher pH values (Figure 6). Lu^{3+} bound to the C2 domain, as indicated by cation-induced changes in intrinsic Trp^{71} fluorescence, yielding an average (±SEM, n = 3) $[Lu^{3+}]_{1/2}$ value of 2.1 ± 0.4 μM and a Hill coefficient of 2.3 ± 0.2. Ca^{2+} also bound cooperatively to the cPLA$_2$-α C2 domain under these conditions, yielding a Hill coefficient of 1.9 ± 0.2. However, the $[Ca^{2+}]_{1/2}$ value equal to 35 ± 2 μM observed at pH 6.0 was significantly greater than the value of 11 μM measured at pH 7.0 (Table 1). Similarly, Ca^{2+} also induced membrane docking under these conditions in the FRET assay (Figure 6B), yielding a Hill coefficient of 1.5 ± 0.1 and a $[Ca^{2+}]_{1/2}$ value of 16.6 ± 0.8 μM, which was also greater than the value of 2 μM measured at pH 7.0 (Table 1). Like Ca^{2+}, Lu^{3+} induced docking of the C2 domain to PC membranes (Figure 6B), but the sub-micromolar apparent affinity of binding was too high to allow accurate determination of the $[Lu^{3+}]_{1/2}$ and Hill coefficient required for membrane docking. Other trivalent cations, including the group IIIB ion La^{3+} and the lanthanide ions Nd^{3+} and Gd^{3+}, also bound to the cPLA$_2$-α C2 domain and induced membrane docking at sub-micromolar concentrations (data not shown). These results indicate that trivalent cations can bind to the isolated cPLA$_2$-α C2 domain with a stoichiometry of at least two, in some cases with higher affinity than Ca^{2+}, and can functionally replace Ca^{2+} to induce membrane docking.

DISCUSSION

These results demonstrate that a combination of cation charge and size constraints in the Ca^{2+}-binding site shapes the strong Ca^{2+} selectivity of the cPLA$_2$-α C2 domain. These constraints enable the domain to bind to mobilized Ca^{2+} generated during cellular activation while immersed in high cytoplasmic concentrations of other physiological cations. The fundamental principles underlying these constraints play an important role in shaping the cation affinity and selectivity not only of C2 domains but also of other Ca^{2+}-binding proteins, including EF-hands, and of synthetic organic chelators (reviewed in refs *33* and *38*). In contrast to the EF-hand and other Ca^{2+}-binding motifs characterized to date, however, the two Ca^{2+} ions that bind with positive cooperativity to the C2 motif are located immediately adjacent to one another. In the cPLA$_2$-α C2 domain, the center-to-center distance of the two Ca^{2+} ions is only 4.2 Å (*6*). These results suggest that two metal ions are essential for stable docking to target membranes. These conclusions likely can be generalized to other C2 domains, since similarities in divalent cation selectivity by different C2 domains have been noted (*14*−*17*, *39*). The following discussion will focus on both the equilibrium and kinetic features of metal ion and membrane binding to the cPLA$_2$-α C2 domain.

Cation Binding to the Free cPLA$_2$-α C2 Domain. The kinetic scheme for divalent cation binding to the free cPLA$_2$-α C2 domain is represented by a sequential, two-step mechanism originally proposed for Ca^{2+} binding (*9*):

Scheme 1

$$\text{step 1} \qquad C2 + Me \underset{k_{-1}}{\overset{k_1}{\rightleftharpoons}} C2{\cdot}Me_1$$

$$\text{step 2} \qquad C2{\cdot}Me_1 + Me \underset{k_{-2}}{\overset{k_2}{\rightleftharpoons}} C2{\cdot}Me_1{\cdot}Me_2$$

where steps 1 and 2 represent the sequential macroscopic binding of two metal ions (Me) to the free C2 domain. The order of metal ion binding is indicated by subscripts, where Me_1 represents the first ion to bind and the last to dissociate, governed by forward and reverse rate constants k_1 and k_{-1}, respectively. Evidence that the cPLA$_2$-α C2 domain binds Ca^{2+} with a stoichiometry of two ions per free domain has been provided by a variety of approaches (*6*−*9*), including the Hill coefficient of 1.8 obtained in this study. Similarly, the Hill coefficient of 1.4 measured in this study for Sr^{2+}

binding to the free domain suggests a stoichiometry of two ions per domain, as detailed by the two steps in Scheme 1. By contrast, the measured Hill coefficient of 1.0 for Ba^{2+} suggests a stoichiometry of just one per domain for this ion, as indicated by the first step of Scheme 1. For both Ca^{2+} and Sr^{2+}, the highly cooperative binding indicates that the $C2{\cdot}Me_2$ species is much more stable than $C2{\cdot}Me_1$ such that the latter does not accumulate to a great extent. Further evidence for this picture is provided by the observation that the irreversible dissociation of the two Ca^{2+} or Sr^{2+} ions upon rapid mixing with EDTA (or Quin-2) follows a monoexponential time course, indicating that the two ions dissociate virtually simultaneously in a cooperative manner to yield a single observable step:

Scheme 1a

$$C2{\cdot}Me_1{\cdot}Me_2 \xrightarrow{k_{diss}} C2 + 2Me$$

where k_{diss} represents the observed rate constant for dissociation. In reality, this dissociation must consist of two steps such that the second step is too fast to detect:

Scheme 1b

$$C2{\cdot}Me_1{\cdot}Me_2 \xrightarrow{k_{-2}} C2{\cdot}Me_1 + Me \xrightarrow{k_{-1}} C2 + 2Me$$

where, as above, k_{-2} and k_{-1} represent the dissociation rate constants of the Me_2 and Me_1 ions, respectively. In the framework of the sequential binding model (Scheme 1), this two-step process simplifies to a single observable step (Scheme 1a) when $k_{-1} \gg k_{-2}$, i.e., when the $C2{\cdot}Me_1$ species is much less stable than the $C2{\cdot}Me_2$ species such that dissociation of Me_2 is rate-limiting.

Cation Charge Selectivity of the Free C2 Domain. Comparison of the binding of representative group IA, IIA, and lanthanide cations to the $cPLA_2$-α C2 domain reveals striking charge selectivity of the free domain. The monovalent cations K^+ and Na^+ both fail to induce environmental changes in the C2 domain that increase Trp^{71} emission, fail to induce mobility shifts in the C2 domain subjected to native PAGE, and fail to protect the C2 domain against thermal denaturation, suggesting they are excluded from the C2 domain Ca^{2+}-binding site at concentrations as high as 100−200 mM. In contrast, each of the group IIA cations and representative trivalent cations was able to bind to the C2 domain with millimolar or greater affinity as judged by at least one of these biochemical criteria. K^+ and Na^+, whose effective ionic radii (EIR) are 1.12 and 1.46 Å for 7-fold coordination (*33*), respectively, are similar in size to Ca^{2+} and Ba^{2+} whose EIR are 1.06 and 1.38 Å, respectively. The failure of the former monovalent cations to bind to the free C2 domain (step 1, Schemes 1−3) is proposed to arise from their lack of sufficient charge for stabilizing the close packing of coordinating protein oxygens that must occur as the cation binds to the metal binding cleft of the C2 domain. Sufficient negative charge density is present on these oxygens for accommodation of the binding of two divalent or trivalent cations as indicated by the Hill coefficients for Ca^{2+}, Sr^{2+}, and Lu^{3+}. The higher charge densities of divalent and trivalent cations are able to overcome the considerable electrostatic repulsion between coordinating oxygens as they pack around the bound metal ions. This "electrostatic repulsion" model of charge selectivity by the $cPLA_2$-α C2 domain is illustrated in Figure 7.

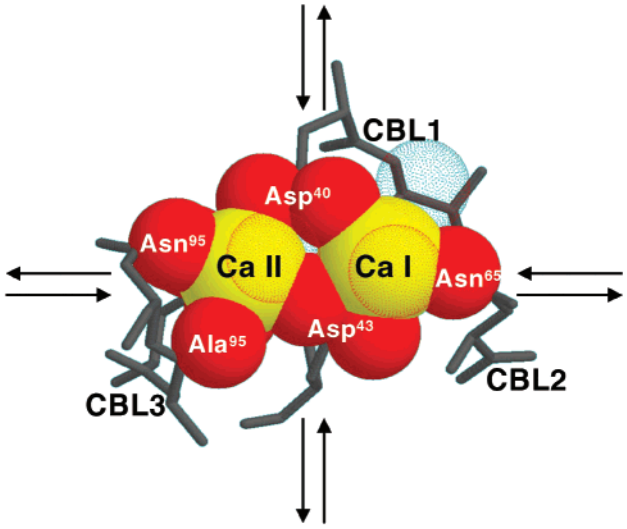

FIGURE 7: Electrostatic repulsion and size exclusion models of cation selectivity proposed for the $cPLA_2$-α C2 domain. Representation of the Ca^{2+}-binding site of the $cPLA_2$-α C2 domain (*6*), where coordinating oxygens are represented by solid red spheres and dot surfaces indicate three ordered water molecules occupying the solvent-exposed coordination positions of the bound Ca^{2+} ions (yellow spheres). The following events are proposed to occur prior to and during cation-triggered membrane docking. In the absence of bound cations, electrostatic repulsion (arrows pointing outward) between oxygens in the site destabilizes the CBLs which as a result are relatively dynamic. Unlike monovalent cations, di- and trivalent spherical cations are able to bind to the site, overcoming this repulsion and immobilizing the CBLs. The first multivalent ion binds at site II, and then the second binds at site I. Binding of Mg^{2+} in site II is relatively unfavorable because the compression of the site to accommodate this small ion is opposed by the repulsion between the coordinating oxygens, and because dehydration of this small ion is energetically costly. At the other end of the size selectivity spectrum, a second Ba^{2+} ion fails to bind because the large Ba^{2+} ion in site II overlaps or distorts the coordinating oxygen array in site I. When multivalent cations of acceptable size are bound, favorable electrostatic contacts between the cations and coordinating oxygens (arrows pointing inward) stabilize the CBLs in the conformation appropriate for membrane docking. Cations whose radii are too large for the site are excluded by the forces of steric strain (again, arrows pointing inward) which restrict the volume available for ion binding. When two multivalent cations of acceptable size occupy the site, hydrophobic groups on the CBLs are properly positioned for insertion into the hydrocarbon phase of the lipid bilayer. Subsequent membrane docking replaces the indicated water molecules with coordinating phospholipid oxygens.

Divalent Cation Size Selectivity of the Free C2 Domain. Each of the group IIA cations is able to bind to the free $cPLA_2$-α C2 domain in solution. However, these divalent cations differ markedly in potency and in the metal stoichiometry that can be achieved in the micromolar range. Although Mg^{2+} concentrations of >1 mM induce an increase in Trp^{71} emission, 1 mM Mg^{2+} fails to induce the electrophoretic mobility shift and to stabilize the domain against thermal denaturation. By contrast, the larger divalent cations Ca^{2+}, Sr^{2+}, and Ba^{2+} each bind to the free C2 domain with low micromolar affinity. The $[Ca^{2+}]_{1/2}$ value for binding to the isolated $cPLA_2$-α C2 domain based on Trp^{71} fluorescence is only 3-fold lower than the $[Sr^{2+}]_{1/2}$ value and is essentially

identical to the $[Ba^{2+}]_{1/2}$ value, suggesting that the C2 domain binds at least one ion of Ca^{2+}, Sr^{2+}, and Ba^{2+} with roughly similar affinities. These results indicate that for divalent cations with effective ionic radii exceeding 0.8 Å, the EIR of Mg^{2+}, at least one ion can bind to the site with little size selectivity in the absence of membranes (step 1, Schemes 1−3).

As noted above, among the group IIA cations, only Ca^{2+} and Sr^{2+} appear to achieve a stoichiometry of two in the micromolar range in the absence of membranes, suggesting that only these ions can fill the second metal ion site efficiently (step 2, Scheme 1). Indeed, in the absence or presence of membranes, the Ba^{2+} fluorescence titration data (Figure 4D) are well-approximated by saturable binding to a single, independent site with a dissociation constant of 15 ± 2 μM (data not shown). Thus, in the micromolar range, the size of the cation-binding site of the free cPLA$_2$-α C2 domain is restricted to exclude even a single Mg^{2+} ion, is restricted to include only one Ba^{2+} ion, but easily accommodates two Ca^{2+} or Sr^{2+} ions. The effective ionic radii of these ions for 7-fold coordination are 0.8 Å (Mg^{2+}), 1.06 Å (Ca^{2+}), 1.21 Å (Sr^{2+}), and 1.38 Å (Ba^{2+}) (*33*). These results indicate that the optimal radius for the second ion is approximately 1.1 Å and that ions with radii much greater than 1.2 Å are excluded (step 2, Scheme 1). The exclusion of the physiological ion Mg^{2+} not only arises from its small size, which is presumed to prevent optimal contacts with the coordinating oxygen array, but also must stem in part from its large free energy of dehydration (*33*). This "size exclusion" model of divalent cation selectivity is illustrated in Figure 7. The nearly total exclusion of the second Ba^{2+} ion arises only from its large size, which is presumed to exceed the volume capacity of the coordinating oxygen array already occupied by one large Ba^{2+} ion. Comparison of the dissociation time courses of Ca^{2+}, Sr^{2+}, and Ba^{2+} provides insights into the relationship between dissociation kinetics and ionic size. As noted above, the rate constant for dissociation of Me_2 limits the dissociation of Me_1 ($k_{-2} \ll k_{-1}$, Scheme 1b) so that monoexponential time courses are observed even when two divalent cations dissociate (Scheme 1a). Since the observed dissociation rate constant is larger for Sr^{2+} than for Ca^{2+} (Table 2), the k_{-2} value for the Me_2 ion appears to increase with increasing divalent cation size. Moreover, the very rapid dissociation of Ba^{2+} relative to that of Ca^{2+} and Sr^{2+} is likely to reflect the very large dissociation rate constants (k_{-1}) of Me_1 ions bound to the site in the absence of Me_2.

Overall, the current working model for the interaction of two medium-sized divalent cations with the free C2 domain proposes that the Me_1 ion first binds weakly and organizes the site to increase the affinity for the Me_2 ion, which subsequently binds and stabilizes the fully occupied site. Subsequently, when the Me_2 ion dissociates, the Me_1 ion follows rapidly due to its lower affinity. The positive cooperativity observed for the binding of Lu^{3+} ions to the free domain suggests that the same model applies to this trivalent lanthanide ion.

Kinetic Scheme for the Binding of Two Multivalent Cations and Subsequent Membrane Docking. A three-step kinetic scheme is required to describe the metal ion-induced docking of the cPLA$_2$-α C2 domain to phospholipid membranes (PL):

Scheme 2

$$\text{step 1} \quad C2 + Me \underset{k_{-1}}{\overset{k_1}{\rightleftharpoons}} C2{\cdot}Me_1$$

$$\text{step 2} \quad C2{\cdot}Me_1 + Me \underset{k_{-2}}{\overset{k_2}{\rightleftharpoons}} C2{\cdot}Me_1{\cdot}Me_2$$

$$\text{step 3} \quad C2{\cdot}Me_1{\cdot}Me_2 + PL \underset{k_{-3}}{\overset{k_3}{\rightleftharpoons}} C2{\cdot}Me_1{\cdot}Me_2{\cdot}PL$$

where steps 1 and 2 represent the sequential binding of two medium-sized divalent or trivalent cations to the free C2 domain and are identical to those in Scheme 1. Step 3 represents the formation of the high-affinity domain−membrane ternary complex ($C2{\cdot}Me_1{\cdot}Me_2{\cdot}PL$) with forward and reverse rate constants of k_3 and k_{-3}, respectively. Evidence that two multivalent cations ions bind cooperatively to the free C2 domain prior to membrane docking is discussed above; moreover, Ca^{2+} and Sr^{2+} each exhibit biexponential kinetics when dissociating from the membrane-bound complex, confirming that two ions remain bound to the domain when docked to the membrane. These findings reinforce the previous direct stoichiometry measurement of two ions per membrane-bound domain for Ca^{2+} (*9*).

In principle, one must also consider other kinetic schemes for metal-stabilized membrane docking in which one or both metal ions can bind after the unsaturated domain is weakly bound to the membrane. In fact, the slow biexponential dissociation of two Ca^{2+} or Sr^{2+} ions from the membrane-bound domain indicates that one ion leaves before the domain fully dissociates from the membrane, supporting the idea that a domain occupied by a single divalent cation can be weakly membrane-bound. Therefore, an alternative pathway for metal ion-induced docking of the cPLA$_2$-α C2 domain to phospholipid membranes could be proposed:

Scheme 3

$$\text{step 1} \quad C2 + Me \underset{k_{-1}}{\overset{k_1}{\rightleftharpoons}} C2{\cdot}Me_1$$

$$\text{step 2} \quad C2{\cdot}Me_1 + PL \underset{k_{-2}}{\overset{k_2}{\rightleftharpoons}} C2{\cdot}Me_1{\cdot}PL$$

$$\text{step 3} \quad C2{\cdot}Me_1{\cdot}PL + Me \underset{k_{-3}}{\overset{k_3}{\rightleftharpoons}} C2{\cdot}Me_1{\cdot}Me_2{\cdot}PL$$

where rate constants for steps 2 and 3 are not identical to those depicted in Scheme 2. Whether $C2{\cdot}Me_1$ first binds Me_2 before binding membranes (k_2, Scheme 2) or first binds PL before binding Me_2 (k_2, Scheme 3) depends on the relative rates of these two competing steps, which in turn depend on the rate constants of the steps and the concentrations of metal ions and membranes. In general, Scheme 2 is expected to dominate for metal ions such as Ca^{2+}, Sr^{2+}, and Lu^{3+} that exhibit strong positive cooperativity in binding to the free domain, since for these metals the concentration of $C2{\cdot}Me_1$ will generally be much lower than that of $C2{\cdot}Me_2$. This picture is further supported by the observation that the domain saturated with a single bound divalent cation at micromolar Ba^{2+} concentrations exhibits little membrane affinity, while much higher Ba^{2+} concentrations yield weak membrane docking presumably by driving the binding of a second Ba^{2+} ion (Table 1 and Figure 4A).

Overall, the evidence strongly suggests that two multivalent cations bind to the free domain prior to membrane docking, and that no additional ions are bound after docking. Moreover, the relative affinities observed for binding of *two* multivalent ions to the free domain are similar to the relative potencies of these ions when used to drive membrane docking (in both cases, $Lu^{3+} > Ca^{2+}$, $Sr^{2+} \gg Mg^{2+}$, Ba^{2+}). It follows that the free domain largely controls metal binding stoichiometry and selectivity, which is established prior to the membrane docking event. Minor additional modulation of selectivity is provided by the protein−membrane interaction, since the ratio of Ca^{2+} to Sr^{2+} affinities increases 2-fold in the presence of membranes.

Different Membrane Affinities of the Domain Loaded with Two Cations. Even in the presence of saturating concentrations of divalent cations, the Ca^{2+}-loaded C2 domain binds to PC membranes with 4-fold higher affinity than the Sr^{2+}-loaded C2 domain, due at least in part to the longer membrane-bound lifetime of the Ca^{2+}-loaded domain. This membrane affinity difference likely arises from the fact that the metal-binding loops of the cPLA$_2$-α C2 domain interact directly with the membrane surface (*7*, *24*, *36*). The different membrane affinities of the ion-saturated domain suggest that either (i) the protein-bound metal ions themselves directly contact the membrane, thereby modulating the nature of the protein−membrane interaction, or (ii) the conformations of the membrane-docked Ca^{2+} binding loops differ when occupied with various divalent cations. The former possibility is consistent with the observation that Ca^{2+} bound to the isolated C2 domain is partially exposed to solvent, where coordinating water molecules could be displaced by headgroup oxygens upon docking to a phospholipid bilayer. Moreover, direct headgroup coordination of the protein-bound Ca^{2+} ions has been observed in the crystal structure of the complex between the PKC-α C2 domain and a short chain lipid (*21*). The latter possibility is consistent with the presence of numerous hydrophobic residues of the cPLA$_2$-α Ca^{2+}-binding loops that are exposed to solution such that conformational rearrangements of these loops could occur upon membrane docking. These possibilities are widely relevant to Ca^{2+}-dependent membrane-binding C2 domains, which all appear to contact membranes through their Ca^{2+}-binding loops (discussed in ref *12*).

Comparison to Other C2 Domains. The C2 domain Ca^{2+}-binding site binds multiple Ca^{2+} ions in a positively cooperative manner, thus enabling the domain to respond to small changes in intracellular Ca^{2+} concentrations, a feature exhibited by many Ca^{2+}-binding signaling proteins (*33*, *38*). Four distinct sites appear to be occupied to varying extents in different C2 domains. Sites II−IV are utilized in the Syt-IA and PKC-*β* C2 domains; sites I−III are utilized in phospholipase C-*δ*1 (PLC-*δ*1), whereas only sites I and II are occupied in cPLA$_2$-α (*4*) (see Figure 7). We hypothesize that in the cPLA$_2$-α C2 domain and all other C2 domains, Ca^{2+} binds first to site II (step 1, Schemes 1−3), since (i) this site is the sole site occupied in crystals of the synaptotagmin C2A domain (*3*), (ii) NMR studies have indicated that this site fills first in the Syt-IA and PKC-*β* C2 domain (*5*, *40*, *41*), (iii) the coordinating ligands in this site, but not others, are strictly conserved throughout Ca^{2+}-dependent C2 domains (*1*), and (iv) binding measurements have indicated remarkably similar affinities (∼20−60 *μ*M) for the binding of the first Ca^{2+} ion to each of the cPLA$_2$-α, PKC-*β*, and Syt-IA C2 domains in the absence of membranes (*12*, *19*, *40*, *41*). Upon occupation of the first Ca^{2+} ion in site II, the occupancy at other sites depends on the given C2 domain. For cPLA$_2$-α, only site I is occupied by the second Ca^{2+} ion (step 2, Schemes 1 and 2, and step 3, Scheme 3), since sites III and IV are inactivated by substitution of Asn for Asp (at position 95) and Val for Ser (at position 97), respectively. For PLC-*δ*1, both sites I and III are occupied after site II. In Syt-IA and PKC-*β*, site I is inactivated due to substitution of a Lys for Asn (corresponding to Asn-65 in cPLA$_2$-α) in the second Ca^{2+}-binding loop; thus, sites III and IV are filled after site II. On the basis of the sequence alignment of the C2 domain (*1*), most other C2 domains that have been reported to bind phospholipid membranes in a Ca^{2+}-dependent manner are predicted to coordinate Ca^{2+} in a fashion similar to that of the PKC-*β* and Syt-IA C2 domains.

Mechanism of Ca^{2+}-Triggered Membrane Docking. Figure 7 illustrates a model for the mechanism of Ca^{2+}-triggered membrane docking that incorporates the results presented here. In the apo state of the C2 domain, the strong electrostatic repulsion between the coordinating oxygens concentrated in the Ca^{2+}-binding cleft destabilizes the loops and increases their inherent flexibility. Greater flexibility is supported by the lower thermal stability of the domain in the absence of bound cations (present report and refs *34* and *35*), a considerable increase in average temperature factors in loop regions in the crystal structures of apo-C2 domains (*42*), and greater flexibility in the loops of the apo-C2 domain of the Syt-IA C2 domain observed by NMR spectroscopy (*5*). Monovalent ions are excluded because their lower charge density is unable to overcome the strong electrostatic repulsion of the coordinating oxygens when they closely pack around the metal. Mg^{2+} is excluded because it is too small for the coordination cavity, preventing the optimal metal−oxygen contacts, and due to its greater dehydration free energy. The first Ca^{2+}, Sr^{2+}, Ba^{2+}, or Lu^{3+} ion binds to site II with relatively low affinity because of the inherent flexibility of the metal-binding loops in the apo state. The binding of this first multivalent cation organizes the site by partially neutralizing the negative charge in the site and thus constraining the flexible loops. The partial stabilization of the loops by cation binding constitutes initiation of the "conformational change" that induces environmental changes transmitted to Trp^{71} in the cPLA$_2$-α C2 domain, ∼12 Å from the Ca^{2+}-binding cleft. A second identical Ca^{2+}, Sr^{2+}, or Lu^{3+} ion binds to site I immediately adjacent to the first ion (approximately 4 Å away, center-to-center distance) in a positively cooperative manner due to the favorable preorientation of ligand oxygens that coordinate it. For Ba^{2+}, the binding of the first ion partially stabilizes the C2 domain as measured by increased thermal stability and environmental changes transmitted to the environment of the buried Trp^{71}. However, this larger Ba^{2+} ion occludes or distorts the second site, yielding half-occupancy.

Membrane docking is triggered by the occupancy of the cleft with two multivalent cations, which alter the local electrostatics, immobilize the loops, and create a stable membrane docking surface composed of the Ca^{2+}-binding loops and the metal ions themselves. The two bound ions are occluded in the C2 domain−membrane complex, either

by steric blockage of the pathway for metal ion dissociation or by direct metal ion coordination by oxygens of the phospholipid headgroup. The C2 domain binds to the membrane surface through variable portions of the Ca^{2+}-binding loops (reviewed in ref *36*). For the cPLA$_2$-α C2 domain, several hydrophobic side chains are oriented favorably for interactions with membranes, highlighting the importance of hydrophobic interactions between this C2 domain and PC membranes (reviewed in ref *12*). For other C2 domains such as those in PKC-*β* and Syt-IA, a substantial decrease in negative surface potential favors interactions with anionic phospholipids (reviewed in ref *12*).

Comparison to Other Divalent Cation Binding Proteins. Overall, the divalent cation size selectivity of the cPLA$_2$-α C2 domain is novel, being intermediate between those of nonselective Mg^{2+}-binding sites such as that of the CheY protein and strongly selective Ca^{2+}-binding sites such as those of certain EF-hand proteins. The weak size selectivity of the CheY Mg^{2+}-binding site has been proposed to stem from the surface location of its cluster of coordinating carboxylates where there are few constraints on cavity size and coordination number (*31*). Since the coordination of divalent cation is completed by water molecules, larger cations can simply employ more coordinating water molecules as needed (*31*). By contrast, the most strongly selective EF-hand sites completely surround the coordinated cation with seven oxygen ligands originating from protein side chains and backbone carbonyl groups, providing a fixed cavity size and coordination number (*33*, *38*). The size selectivity of the C2 domain exhibits features of both prototypical metal binding sites. Mg^{2+} ions are excluded, as in the EF-hand motif, whereas the first binding event shows little discrimination between Ca^{2+}, Sr^{2+}, and Ba^{2+}, as in the CheY site. It follows that the ion binding cavity of the first C2 domain site cannot be configured to provide the 6-fold coordination preferred by Mg^{2+}, but does allow for adequate coordination for metals the size of Ca^{2+} and larger.

Conclusion. Cation charge and size constraints ensure that the cPLA$_2$-α C2 domain can act as a Ca^{2+}-regulated "on−off" switch for membrane targeting in a physiological setting. The capacity of the domain to bind two multivalent cations of the appropriate size is governed primarily by the C2 domain itself rather than by the target membrane, since the free domain selectively binds only certain multivalent cations with a stoichiometry of two, and this same selectivity is observed in cation-triggered membrane docking. The physical origins of the ionic charge and size constraints will require further investigation to determine the contribution of individual residues in shaping the ion selectivity and affinity of the C2 domain Ca^{2+}-binding site. Potentially, cation size and charge constraints also shape the Ca^{2+} selectivity and affinity in other C2 domains, where they are likely to vary considerably given reported differences in Ca^{2+} binding stoichiometry, affinity, cooperativity, and kinetics. These varying constraints are likely to have arisen from the functional specialization of different C2 domains which leads to the expansion of the repertoire of signaling roles carried out by C2 domain proteins (*12*).

REFERENCES

1. Nalefski, E. A., and Falke, J. J. (1996) *Protein Sci. 5*, 2375−2390.
2. Rizo, J., and Südhof, T. C. (1998) *J. Biol. Chem. 273*, 15879−15882.
3. Sutton, R. B., Davletov, B. A., Berghuis, A. M., Südhof, T. C., and Sprang, S. R. (1995) *Cell 80*, 929−938.
4. Sutton, R. B., and Sprang, S. R. (1998) *Structure 6*, 1395−1405.
5. Shao, X., Fernandez, I., Südhof, T. C., and Rizo, J. (1998) *Biochemistry 37*, 16106−16115.
6. Perisic, O., Fong, S., Lynch, D. E., Bycroft, M., and Williams, R. L. (1998) *J. Biol. Chem. 273*, 1596−1604.
7. Xu, G. Y., McDonagh, T., Yu, H. A., Nalefski, E. A., Clark, J. D., and Cumming, D. A. (1998) *J. Mol. Biol. 280*, 485−500.
8. Dessen, A., Tang, J., Schmidt, H., Stahl, M., Clark, J. D., Seehra, J., and Somers, W. S. (1999) *Cell 97*, 349−360.
9. Nalefski, E. A., Slazas, M. M., and Falke, J. J. (1997) *Biochemistry 36*, 12011−12018.
10. Nalefski, E. A., Sultzman, L. A., Martin, D. M., Kriz, R. W., Towler, P. S., Knopf, J. L., and Clark, J. D. (1994) *J. Biol. Chem. 269*, 18239−18249.
11. Nalefski, E. A., McDonagh, T., Somers, W., Seehra, J., Falke, J. J., and Clark, J. D. (1998) *J. Biol. Chem. 273*, 1365−1372.
12. Nalefski, E. A., Wisner, M. A., Chen, J. Z., Sprang, S. R., Fukuda, M., Mikoshiba, K., and Falke, J. J. (2001) *Biochemistry 40*, 3089−3100.
13. Alberts, B., Bray, D., Lewis, J., Raff, M., Roberts, K., and Watson, J. D. (1994) *Molecular Biology of the Cell*, 3rd ed., Garland Publishing, Inc., New York.
14. Davletov, B. A., and Südhof, T. C. (1993) *J. Biol. Chem. 268*, 26386−26390.
15. Fukuda, M., Kojima, T., and Mikoshiba, K. (1997) *Biochem. J. 323*, 421−425.
16. Davletov, B. A., and Südhof, T. C. (1994) *J. Biol. Chem. 269*, 28547−28550.
17. Li, C., Davletov, B. A., and Südhof, T. C. (1995) *J. Biol. Chem. 270*, 24898−24902.
18. Reynolds, L. J., Hughes, L. L., Louis, A. I., Kramer, R. M., and Dennis, E. A. (1993) *Biochim. Biophys. Acta 1167*, 272−280.
19. Davis, A. F., Bai, J., Fasshauer, D., Wolowick, M. J., Lewis, J. L., and Chapman, E. R. (1999) *Neuron 24*, 363−376.
20. Tocanne, J. F., and Teissie, J. (1990) *Biochim. Biophys. Acta 1031*, 111−142.
21. Verdaguer, N., Corbalan-Garcia, S., Ochoa, W. F., Fita, I., and Gomez-Fernandez, J. C. (1999) *EMBO J. 18*, 6329−6338.
22. Clark, J. D., Lin, L. L., Kriz, R. W., Ramesha, C. S., Sultzman, L. A., Lin, A. Y., Milona, N., and Knopf, J. L. (1991) *Cell 65*, 1043−1051.
23. Evans, J. H., Spencer, D. M., Zweifach, A., and Leslie, C. C. (2001) *J. Biol. Chem. 276*, 30150−30160.
24. Perisic, O., Paterson, H. F., Mosedale, G., Lara-Gonzalez, S., and Williams, R. L. (1999) *J. Biol. Chem. 274*, 14979−14987.
25. Clark, J. D., Schievella, A. R., Nalefski, E. A., and Lin, L. L. (1995) *J. Lipid Mediators Cell Signalling 12*, 83−117.
26. Kramer, R. M., and Sharp, J. D. (1997) *FEBS Lett. 410*, 49−53.
27. Gijon, M. A., and Leslie, C. C. (1999) *J. Leukocyte Biol. 65*, 330−336.
28. Kotake, S., Hey, P., Mirmira, R. G., and Copeland, R. A. (1991) *Arch. Biochem. Biophys. 285*, 126−133.
29. Nalefski, E. A., and Falke, J. J. (2001) in *Methods in Molecular Biology: Calcium-Binding Protein Protocols* (Vogel, H. J., Ed.) Vol. 1, Chapter 19, Humana Press, Totowa, NJ.
30. Grabarek, Z., and Gergely, J. (1983) *J. Biol. Chem. 258*, 14103−14105.
31. Needham, J. V., Chen, T. Y., and Falke, J. J. (1993) *Biochemistry 32*, 3363−3367.
32. Tonomura, B., Nakatani, H., Ohnishi, M., Yamaguchi-Ito, J., and Hiromi, K. (1978) *Anal. Biochem. 84*, 370−383.
33. Falke, J. J., Drake, S. K., Hazard, A. L., and Peersen, O. B. (1994) *Q. Rev. Biophys. 27*, 219−290.
34. Shao, X., Li, C., Fernandez, I., Zhang, X., Südhof, T. C., and Rizo, J. (1997) *Neuron 18*, 133−142.

35. Garcia-Garcia, J., Corbalan-Garcia, S., and Gomez-Fernandez, J. C. (1999) *Biochemistry 38*, 9667−9675.
36. Nalefski, E. A., and Falke, J. J. (1998) *Biochemistry 37*, 17642−17650.
37. Wu, P., and Brand, L. (1994) *Anal. Biochem. 218*, 1−13.
38. Linse, S., and Forsen, S. (1995) *Adv. Second Messenger Phosphoprotein Res. 30*, 89−151.
39. Sugita, S., Hata, Y., and Südhof, T. C. (1996) *J. Biol. Chem. 271*, 1262−1265.
40. Shao, X., Davletov, B. A., Sutton, R. B., Südhof, T. C., and Rizo, J. (1996) *Science 273*, 248−251.
41. Ubach, J., Zhang, X., Shao, X., Südhof, T. C., and Rizo, J. (1998) *EMBO J. 17*, 3921−3930.
42. Essen, L. O., Perisic, O., Lynch, D. E., Katan, M., and Williams, R. L. (1997) *Biochemistry 36*, 2753−2762.

BI011798H